Title

Quantification of lipoprotein lipase in mouse plasma with a sandwich enzyme-linked immunosorbent assay.

Journal

Journal of Lipid Research, 65(4)

Authors

Kimura, Takao
Miyashita, Kazuya
Fukamachi, Isamu
et al.

Publication Date

2024-04-11

DOI

10.1016/j.jlr.2024.100532

Peer reviewed

JLR METHODS

Quantification of lipoprotein lipase in mouse plasma with a sandwich enzyme-linked immunosorbent assay

Takao Kimura[1,2]*, Kazuya Miyashita[3], Isamu Fukamachi[3], Kumiko Fukamachi[3], Kazumi Ogura[3], Erina Yokoyama[3], Katsuhiko Tsunekawa[1,2], Takumi Nagasawa[1,2], Michael Ploug[4,5], Ye Yang[6], Wenxin Song[6], Stephen G. Young[6,7], Anne P. Beigneux[6], Katsuyuki Nakajima[1], and Masami Murakami[1,2]

[1]Department of Clinical Laboratory Medicine, Gunma University Graduate School of Medicine, Maebashi, Gunma, Japan; [2]Clinical Laboratory Center, Gunma University Hospital, Maebashi, Gunma, Japan; [3]Immuno–Biological Laboratories, Fujioka, Gunma, Japan; [4]Finsen Laboratory, Copenhagen University Hospital - Rigshospitalet, Copenhagen, Denmark; [5]Biotech Research and Innovation Centre, University of Copenhagen, Copenhagen, Denmark; [6]Department of Medicine, and [7]Department of Human Genetics, David Geffen School of Medicine, University of California, Los Angeles, CA, USA

Abstract To support in vivo and in vitro studies of intravascular triglyceride metabolism in mice, we created rat monoclonal antibodies (mAbs) against mouse LPL. Two mAbs, mAbs 23A1 and 31A5, were used to develop a sandwich ELISA for mouse LPL. The detection of mouse LPL by the ELISA was linear in concentrations ranging from 0.31 ng/ml to 20 ng/ml. The sensitivity of the ELISA made it possible to quantify LPL in serum and in both pre-heparin and post-heparin plasma samples (including in grossly lipemic samples). LPL mass and activity levels in the post-heparin plasma were lower in *Gpihbp1*$^{-/-}$ mice than in wild-type mice. In both groups of mice, LPL mass and activity levels were positively correlated. Our mAb-based sandwich ELISA for mouse LPL will be useful for any investigator who uses mouse models to study LPL-mediated intravascular lipolysis.

Supplementary key words lipids • triglycerides • transport • vascular biology • LPL • HTGL • GPIHBP1

The lack of monospecific antibodies has long hampered efforts to understand the mechanisms underlying intravascular triglyceride metabolism (1, 2). We have generated monoclonal antibodies (mAbs) against multiple proteins in plasma triglyceride metabolism (3–5), including human LPL (3, 4). We have used the human LPL-specific mAbs to establish immunoassays to measure LPL levels in human plasma and serum samples (3, 4). We have also generated antibodies against human glycosylphosphatidylinositol-anchored high-density lipoprotein binding protein 1 (GPIHBP1) (5), a glycosylphosphatidylinositol-anchored protein of endothelial cells that is responsible for capturing LPL from within the interstitial spaces (where it is secreted by parenchymal cells) and transporting it to the capillary lumen (where it carries out the lipolytic processing of triglyceride-rich lipoproteins in the bloodstream) (2). We have used our GPIHBP1-specific mAbs to create immunoassays to measure levels of human GPIHBP1 in plasma or serum (5).

Here, we report the development of rat mAbs against mouse LPL and the development of an mAb-based sandwich ELISA for mouse LPL. The assay is very sensitive and is useful for measuring mouse LPL levels in serum and in both pre-heparin and post-heparin plasma. With this assay, we were able to document that amounts of LPL in the post-heparin plasma are much lower in *Gpihbp1*$^{-/-}$ mice than in wild-type mice.

MATERIALS AND METHODS

Reagents

Bovine serum albumin (BSA) was purchased from Sigma-Aldrich (Tokyo, Japan). Potential interfering agents including bilirubin F and bilirubin C and hemoglobin were purchased from Sysmex (Kobe, Japan). Triglycerides were purchased from Otsuka Pharmaceutical Co., Ltd. (Tokyo, Japan). All chemicals and reagents were of the highest available grade.

Mice

We used B6D2F1/Crl, BALB/c, and C57BL/6J mice. We also used *Gpihbp1*$^{-/-}$ mice on a C57BL/6J background. All mice were fed a chow diet and housed in a barrier facility with a 12-h light-dark cycle. All animal studies were conducted at the University of California, Los Angeles, CA. All animal

Inquiries regarding the antibodies or the ELISA assay should be addressed to: Masami Murakami. E-mail: mmurakam@gunma-u.ac.jp; Address: Showa-machi 3-39-22, Maebashi, Gunma 371-8511, Japan.
*For correspondence: Takao Kimura, tkimura@gunma-u.ac.jp.

 https://doi.org/10.1016/j.jlr.2024.100532

studies were approved by the Animal Research Committee of University of California, Los Angeles, CA.

Plasma collection and heparin treatment

Mouse blood was collected by retro-orbital bleed. Eight drops of blood were collected from each mouse. Blood samples were centrifuged at 13,000 rpm for 3 min at 4°C, and the supernatant (~150 μl) was stored at −80°C. *Gpihbp1*$^{+/+}$ and *Gpihbp1*$^{-/-}$ mice were given an intravenous injection of heparin (50 U/mouse). Blood samples were collected before and 2 min after the heparin injection (6).

Expression and purification of mouse LPL and human GPIHBP1

Untagged mouse LPL (mLPL) was co-expressed with lipase maturation factor 1 and human GPIHBP1 with an N-terminal uPAR epitope tag (detectable by mAb R24) (7) in *Drosophila* S2 cells; the secreted mLPL was purified to homogeneity by heparin-Sepharose chromatography (8). The mouse LPL contained a single amino acid substitution (p.R324A) to eliminate an unwanted furin cleavage site. Lipase maturation factor 1 and GPIHBP1 were co-expressed with mLPL in *Drosophila* S2 cells to assist with the intracellular folding of mLPL and to prevent unfolding of the metastable LPL during secretion and in the conditioned media, respectively (9). Recombinant human GPIHBP1, used for native PAGE experiments, represents the soluble protein (residues 1–131) without the C-terminal signal sequence that is required for glycolipid membrane anchoring. Soluble GPIHBP1 was expressed in *Drosophila* S2 cells and purified as described (10).

Monoclonal antibodies

Wistar rats were immunized with purified full-length mouse LPL (8). Antibody titers in the plasma of the immunized Wistar rats were monitored by ELISA, and lymphocytes were fused with X63/Ag.8.653 myeloma cells. Hybridomas were grown under azaserine hypoxanthine selection, and ~10,000 hybridoma supernatants were screened by ELISA for high-affinity monoclonal antibodies. The top six clones were expanded and subcloned by serial dilution. Monoclonal antibodies were isotyped with commercially available kits (BD Bioscience, New Jersey), and the hybridomas were adapted to serum-free medium. Two mouse LPL-specific mAbs (23A1 and 31A5) were isolated from the cell culture medium on Protein-G-Sepharose columns (GE Healthcare, Illinois); immunoglobulins were eluted with a 0.1 mol/L citrate buffer (pH 2.5) and then dialyzed against PBS. The protein concentration of the mAbs was estimated from the optical density.

Mapping LPL regions harboring epitopes of mAbs 23A1 and 31A5

The plasmids for the expression of V5/His-tagged mLPL/hLPL hybrid proteins in mammalian cells were previously described (11). CHO cells were electroporated with 5 μg of plasmid DNA using the Amaxa Cell line Nucleofector kit T and a Nucleofector II apparatus (both from Lonza) and then plated in wells of a 24-well tissue culture plate. The next day, the cells were washed in PBS and then collected in RIPA buffer (Millipore Sigma) supplemented with protease inhibitor cocktail tablets (Complete ULTRA tablets, Roche). Total cells lysates were prepared by sonication followed by centrifugation (13,000 rpm, 15 min).

For Western blot analyses, cell lysates were size-fractionated on a 4%–12% Bis-Tris gel, transferred to a sheet of nitrocellulose, blocked in StartingBlock (Pierce), and then incubated with rat mAb 23A1 (20 μg/ml) and a mouse mAb anti-V5 tag (10 μg/ml; Thermo Fisher scientific), followed by incubation with a IRDye800-labeled donkey anti-rat IgG (1:2,000) and a IRDye680-labeled donkey anti-mouse IgG (1:2,000). Antibody signals were detected on an IR scanner (Li-Cor).

For ELISA studies, 96-well plates were coated overnight with 0.5 μg of either mAb 31A5 or a mouse mAb anti-His tag (AbD serotec). After washing in PBS containing 5 U/ml heparin and 0.1% BSA, blocking in StartingBlock (Pierce), 140 μl of total cell lysates diluted 1:3 in StartingBlock was applied to the wells and incubated overnight. After washing, an HRP-labeled V5 tag antibody was added to the wells (1:5,000; Thermo Fisher scientific) and incubated at room temperature for 1.5 h. After renewed washing, 50 μl of 1-step Ultra TMB substrate was added (Thermo Fisher scientific) and the reaction proceeded for 5 min at room temperature before it was stopped by adding 50 μl of 2 M sulfuric acid. The absorbance was read at 450 nm on a SpectraMax ID3 plate reader (Molecular Devices).

Immunoprecipitation of mouse LPL

The mouse LPL-specific mAbs (23A1, 31A5) or an anti-mouse pTau mAb were mixed with 50 μl of 153-6046 Affi-Gel 10 (BIO-RAD, Tokyo, Japan) and blocked with ethanolamine. Next, the samples, either recombinant mouse LPL (100 ng) or post-heparin mouse plasma (100 μl), were incubated with the three different antibody-conjugated beads overnight at 4°C. After washing the beads in PBS, the beads were mixed with 2× sample buffer containing 125 mM Tris-Cl (pH 6.8), 4% SDS, 20% glycerol, 10% 2-melcaptoethanol, and 0.02% BPB and then incubated for 3 min at 100°C. The amount of LPL that was immunoprecipitated by the antibody-coated beads was then assessed by Western blotting. The immunoprecipitated material was size-fractioned with 5%–20% gradient polyacrylamide gels (E-D520L, e-PAGEL, ATTO, Tokyo, Japan) and then transferred to PVDF membranes. Membranes were blocked for 1 h and then probed with an HRP-labeled rabbit anti-mouse LPL antibody (0.5 μg/ml) in PBS with 5% skim milk and 0.2% Tween-20. After washing, the blot was visualized using T7101A Western BLoT Chemiluminescence HRP Substrate (Takara Bio, Shiga, Japan).

Native polyacrylamide gel electrophoresis

We used native polyacrylamide gels to test the ability of the rat mAbs to bind to GPIHBP1-bound mouse LPL (12, 13). In brief, 1 μg mLPL or 1 μg mLPL • hGPIHBP1 complexes were pre-incubated with 2.2 μg mAb 23A1 or 2.5 μg mAb 31A5 on ice for 10 min. Stock solution of mLPL-hGPIHBP1 complexes was prepared by incubating 1 mg/ml of both mLPL and hGPIHBP1 on ice for 30 min—corresponding to a 1:3 M ratio of mLPL to hGPIHBP1. The sample mixtures were loaded onto 4%–16% native polyacrylamide gels (Novex, Thermo Fisher Scientific) and then subjected to a field gradient of 100 V for 10 min, 200 V for 30 min, and 300 V for 20 min at 4°C in a Tris-glycine buffer (pH 8.4). To visualize the protein migration pattern, native gels were stained with Coomassie G-250.

An ELISA to detect and measure LPL in mouse plasma

96-well ELISA plates were coated with the anti-mouse LPL mAb 23A1 (1 μg/well) overnight at 4°C. After blocking

overnight at 4°C with PBS containing 1% BSA and 0.05% NaN_3, dilutions of serum (1:50) and post-heparin plasma (1:250) samples (diluted in PBS containing 1% BSA, 0.05% Tween 20, 2 mol/L NaCl, and 0.05% ProClin 300) were added to the wells, and the plates were incubated overnight at 4°C. On the next day, plates were washed, and the captured mouse LPL was detected with 0.5 μg/ml of HRP-labeled anti-mouse LPL mAb 31A5 (diluted in PBS containing 1% BSA, 0.05% Tween 20%, and 0.05% ProClin 300). After a 30-min incubation at 4°C, the plates were washed, and 100 μl of TMB substrate (Kem-En-Tec Nordic A/S, Taastrup, Denmark) were added to each well. Thirty minutes later, the reaction was stopped by adding 100 μl 2 M sulfuric acid. The optical density was read at 450 nm.

Evaluation of LPL and hepatic triglyceride lipase activities

LPL and hepatic triglyceride lipase (HTGL) activities in mouse plasma were measured with the LPL/HTGL activity assay kit from Immuno-Biological Laboratories (Fujioka, Japan). The assay was performed according to the manufacturer's instructions with an auto-analyzer (BIOLIS 24i Premium, Tokyo Boeki Medisys, Tokyo, Japan) (14–16). LPL and HTGL activities were assayed in the presence and absence of apo-CII, an LPL cofactor (14–16). LPL activity was calculated from the total lipase activity in the presence of apo-CII by subtracting the HTGL activity measured in the absence of apo-CII (14–16).

Immunohistochemistry studies

The ability of mAbs 23A1 and 31A5 to detect mLPL was tested on transfected cells and sections of mouse heart. CHO cells were transfected with an expression vector for mLPL and then plated on glass coverslips. The next day, the cell-coated coverslips were fixed in methanol. Frozen heart sections (10-μm–thick) were fixed in 3% paraformaldehyde. After permeabilization in 0.2% Triton X100, samples were blocked in PBS containing 0.2% BSA and 5% donkey serum and then incubated overnight with mAbs 23A1 or 31A5 and the rabbit pAb 3174 against mouse LPL (all at 15 μg/ml). After washing, samples were incubated for 30 min at room temperature with Alexa Fluor 568–labeled donkey anti rabbit IgG (1:200; Thermo Fisher scientific) and DyLight 650–labeled donkey anti rat IgG (1:200; Thermo Fisher scientific). After washing, samples were post-fixed in 3% paraformaldehyde. Cell coverslips were mounted on slides with ProLong Diamond Antifade mountant with DAPI (Thermo Fisher scientific). Images were acquired on a LSM980 Zeiss confocal microscope with a 20× objective lens.

Statistical analysis

Statistical differences in mean values were analyzed with a Student's t test, Welch's t test, or a paired t test. Statistical significance was set at $P < 0.05$.

RESULTS

Rat mAbs against mouse LPL

We developed a panel of six rat mAbs against mouse LPL. To create an immunoassay, we used two mAbs (23A1 and 31A5) with the highest affinity for mouse LPL. mAbs 23A1 (IgG2b-k) and 31A5 (IgG2b-k) bound tightly to native mouse LPL and could be used to immunoprecipitate recombinant mouse LPL as well as the LPL in post-heparin mouse plasma (**Fig. 1**). With native PAGE, we found that mAb 23A1 binds mouse LPL complexed with human GPIHBP1, whereas mAb 31A5 does not (**Fig. 2**). The distinct patterns of 23A1 and 31A5 reactivity for free and GPIHBP1-bound mouse LPL resemble the patterns of mAbs 5D2 and 88B8 for human LPL (11, 12). We further characterized the location of the epitopes for mAb 23A1 (Supplemental Fig. S1) and 31A5 (Supplemental Fig. S2). The epitopes of mAbs 23A1 and 31A5 are located between mouse LPL amino acid residues 369 and 399 (Supplemental Figs. S1 and S2). Both mAbs 23A1 and 31A5 detect mouse LPL in transfected CHO cells, as judged by immunofluorescence microscopy (Supplemental Fig. S3). Also, mAbs 23A1 and 31A5 are useful for immunohistochemistry studies; both antibodies detect mouse LPL in cryosections of mouse heart (Supplemental Fig. S4).

A sandwich ELISA for mouse LPL

We developed a solid-phase sandwich ELISA for mouse LPL using mAb 23A1 as the capture antibody and HRP-labeled mAb 31A5 as the detecting antibody (the "23/31 ELISA"). While both 23A1 and 31A5 bind between mouse LPL residues 369 and 399, the epitopes for these antibodies do not overlap (making a sandwich ELISA possible). Of note, the crystal structure of LPL (17) revealed that this stretch of 30 amino acids spans surface-exposed regions that occupy opposite sides of LPL's C-terminal domain; thus, it is easy to conceptualize non-overlapping epitopes within this stretch of 30 amino acids.

The 23/31 ELISA was standardized with recombinant mouse LPL, and the working range for the ELISA was 0.31–20 ng/ml (**Fig. 3**A). The analytical limit of quantification for this assay was determined according to

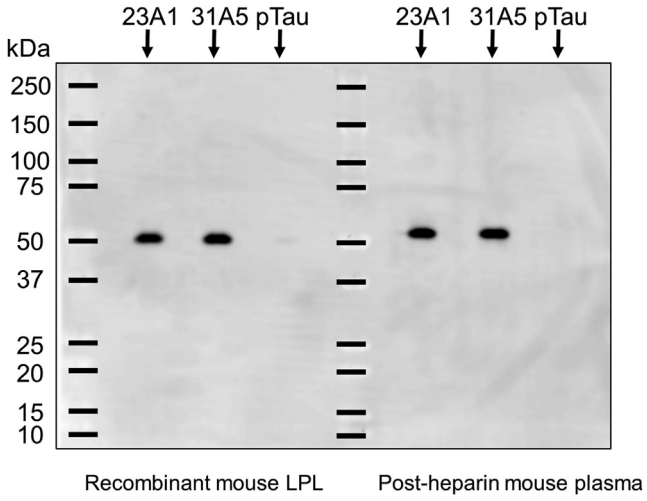

Fig. 1. mAbs 23A1 and 31A5 bind to native mouse LPL. Western blot analysis showing that mAbs 23A1 and 31A5 can be used to immunoprecipitate recombinant mouse LPL (*left panel*) and LPL in mouse post-heparin plasma (*right panel*). An antibody against pTau was used as a negative control.

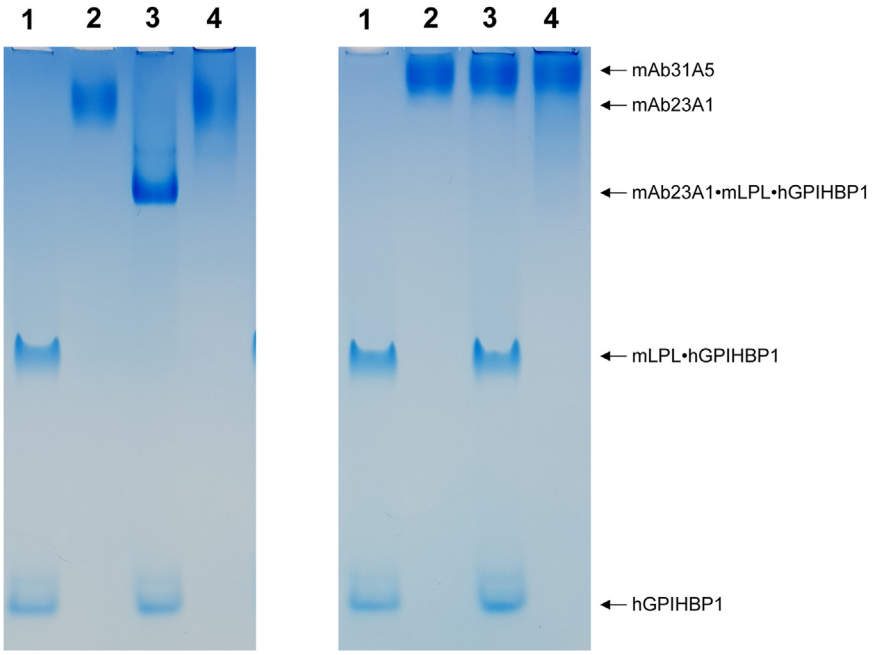

Fig. 2. Native PAGE analysis to test the ability of mAbs 23A1 (*left*) and 31A5 (*right*) to bind to GPIHBP1-bound mLPL. Lane 1: Preformed mLPL • hGPIHBP1 complexes (1 μg) were analyzed alone; lane 2: mLPL mAbs (2–3 μg) alone; lane 3: mLPL mAbs (2–3 μg) in the presence of mLPL • hGPIHBP1 complexes; lane 4: mLPL mAbs (2–3 μg) in the presence of mLPL (no hGPIHBP1). Previous biophysical studies on LPL and its interaction partners have documented the migration patterns of LPL, GPIHBP1, and their complexes in native PAGE (12, 13). mLPL, mouse LPL.

guidelines by the Clinical & Laboratory Standards Institute (18, 19). The limit of sensitivity for the ELISA was 0.036 ng/ml. Because the assay is only linear up to 20 ng/ml, plasma samples must be diluted before performing measurements. We established that dilution curves in the 1:50 to 1:200 range for pre-heparin plasma samples and in the 1:250 to 1:1,000 range for post-heparin plasma samples were parallel to the LPL standard curve, indicating that the ELISA can reliably measure the concentration of LPL in plasma both before (Fig. 3B) and after (Fig. 3C) a bolus of heparin. We established the specificity of the 23/31 ELISA; the ELISA detected mouse LPL but not mouse endothelial lipase or hepatic lipase (Supplemental Fig. S5). The ELISA was capable of measuring levels of LPL in cell lysates and culture medium from mouse myoblast cells (C2C12 cells) (Supplemental Fig. S6).

To assess the intra- and inter-assay variation of the 23/31 ELISA, we established three quality control (QC) mouse LPL samples corresponding to the high, middle, and low regions of the calibration curve. We determined the intra-assay variation with 24 repeated measurements of each QC sample in a plate, and inter-assay variation was determined by assessing each QC sample

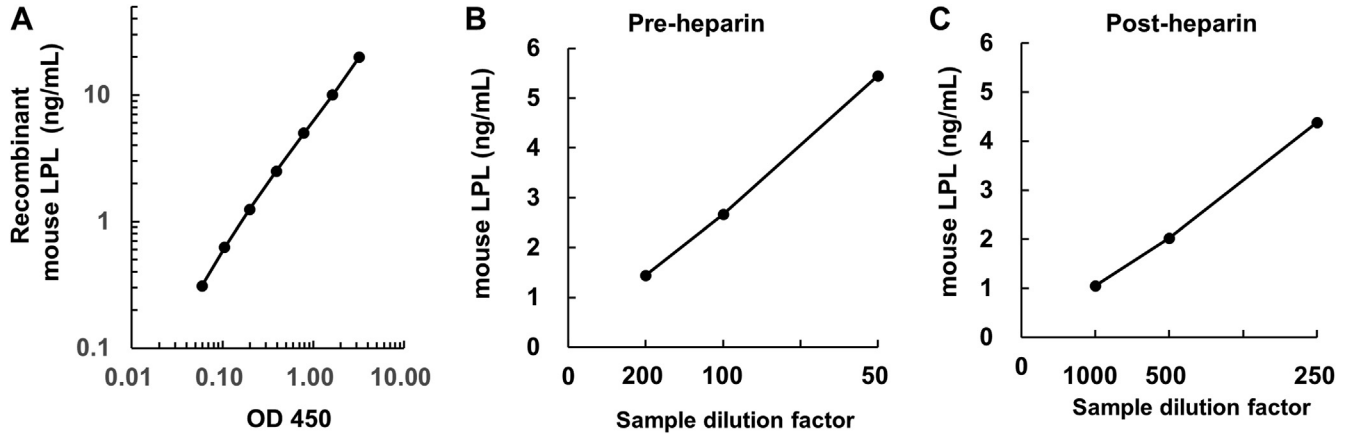

Fig. 3. Linearity of mouse LPL ELISA (the "23/31 ELISA") in which 23A1 was used as the capture antibody and 31A5 was used as the detection antibody. A: Log-log plot of a standard curve of recombinant mouse LPL (range, 0.31–20 ng/ml). B and C: Plots showing linearity of the mouse LPL ELISA over a wide range of 1:2 serial dilutions of serum from C57BL/6J mice before (B) and after (C) a bolus of heparin.

across 13 different plates. The intra-assay coefficient of variation and QC sample concentrations were 6.1% (10.3 ng/ml) in the high, 5.2% (2.24 ng/ml) in the middle, and 5.8% (0.73 ng/ml) in the low region of the calibration curve. The inter-assay coefficient of variation and QC sample concentrations were 4.0% (9.28 ng/ml) in the high, 6.0% (2.00 ng/ml) in the middle, and 10.2% (0.069 ng/ml) in the low region of the calibration curve.

To assess the recovery rate of mouse LPL in the 23/31 ELISA, different amounts of purified recombinant mouse LPL were added to samples, and total amount of mouse LPL in each sample was measured with the ELISA. The recovery rate was determined as the difference between the measured concentration and the theoretical concentration. In plasma samples spiked with recombinant mouse LPL, the recovery of the spiked recombinant LPL ranged from 102% to 105%.

We also evaluated the interference with mouse LPL measurements by bilirubin F, bilirubin C, hemoglobin, heparin, and triglycerides. Bilirubin F and bilirubin C (up to 20 mg/dl), hemoglobin (up to 500 mg/dl), heparin (up to 80,000 ng/ml), and triglycerides (up to 500 mg/dl, in the form of intralipid) did not significantly affect measurements of LPL by the 23/31 ELISA (Supplemental Fig. S7).

Measurement of mouse LPL levels and activities in *Gpihbp1*$^{+/+}$ and *Gpihbp1*$^{-/-}$ mice

Chow-fed *Gpihbp1*$^{-/-}$ mice have milky plasma (**Fig. 4**A) and have been reported to have low plasma LPL levels (2, 20). Using the 23/31 ELISA, we measured pre-heparin and post-heparin plasma LPL concentrations in samples of *Gpihbp1*$^{-/-}$ and *Gpihbp1*$^{+/+}$ mice. Pre-heparin plasma LPL levels were higher in *Gpihbp1*$^{+/+}$ mice than in *Gpihbp1*$^{-/-}$ mice (76.5 ± 15.3 ng/ml vs. 32.0 ± 5.0 ng/ml) (Fig. 4B). As expected, (2, 20), heparin increased plasma LPL levels in *Gpihbp1*$^{+/+}$ mice by more than 30-fold (to 2376.6 ± 260.6 ng/ml) (Fig. 3B). Heparin also increased plasma LPL levels in *Gpihbp1*$^{-/-}$ mice but only by ~8 fold (to 242.2 ± 123.6 ng/ml) (Fig. 4B).

We found no significant differences in the pre-heparin plasma levels of LPL activity in *Gpihbp1*$^{+/+}$ mice (32.8 ± 2.9 U/L) and *Gpihbp1*$^{-/-}$ mice (37.0 ± 9.3 U/L) (Fig. 4C). Heparin treatment increased plasma LPL activity in both *Gpihbp1*$^{+/+}$ and *Gpihbp1*$^{-/-}$ mice (Fig. 4C), but the post-heparin plasma LPL activity in *Gpihbp1*$^{+/+}$ mice (1654.5 ± 68.0 U/L) was far higher than in the *Gpihbp1*$^{-/-}$ mice (254.4 ± 26.1 U/L) (Fig. 4C). Not surprisingly, the measurements of LPL mass in the post-heparin plasma correlated positively with measurements of LPL activity (**Fig. 5**).

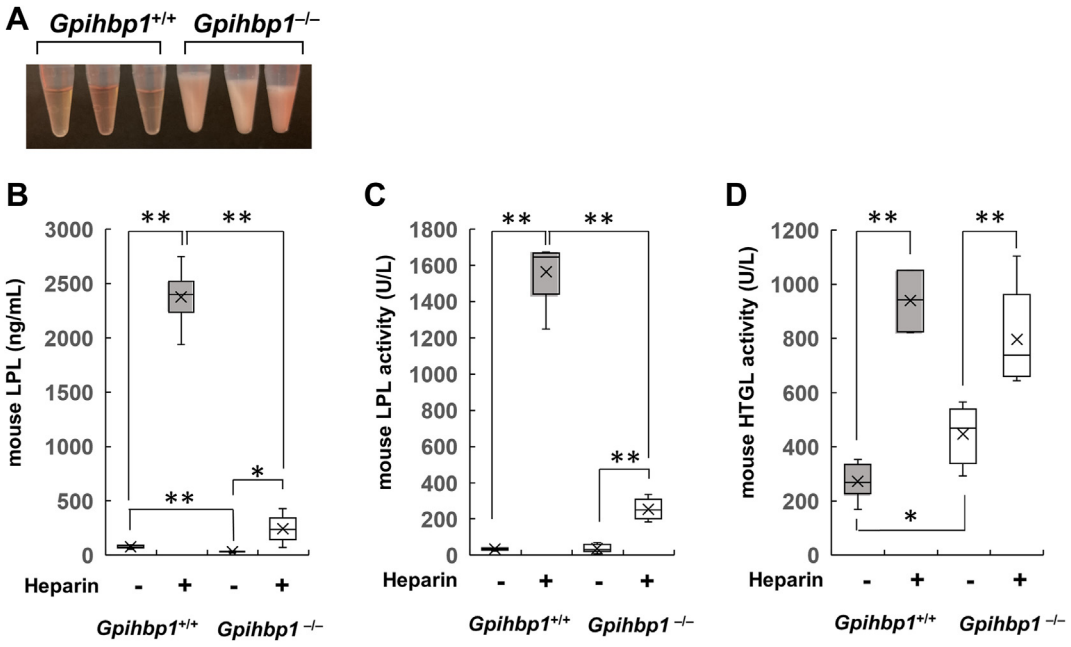

Fig. 4. Plasma LPL levels and activity in *Gpihbp1*$^{+/+}$ and *Gpihbp1*$^{-/-}$ mice. A: Photograph of plasma samples from six 2-month-old littermate chow-fed male *Gpihbp1*$^{+/+}$ and *Gpihbp1*$^{-/-}$ mice. B: LPL mass levels, as judged by the 23/31 ELISA, in the plasma of *Gpihbp1*$^{+/+}$ (*gray* box) and *Gpihbp1*$^{-/-}$ (*white* box) mice before or after heparin treatment. C: Plasma LPL activity in *Gpihbp1*$^{+/+}$ (*gray* box) and *Gpihbp1*$^{-/-}$ (*white* box) mice before or after heparin treatment. D: Plasma HTGL activity in *Gpihbp1*$^{+/+}$ (*gray* box) and *Gpihbp1*$^{-/-}$ (*white* box) mice before or after heparin treatment. Comparison of LPL concentration, LPL activity, and HTGL activity in *Gpihbp1*$^{+/+}$ or *Gpihbp1*$^{-/-}$ mice before and after heparin administration was analyzed with a paired *t* test. Comparison of LPL concentration, LPL activity, and HTGL activity between *Gpihbp1*$^{+/+}$ and *Gpihbp1*$^{-/-}$ mice before or after heparin administration was analyzed with an unpaired *t* test. Data are shown as *box plots*, showing the range, and the first, second, and third quartile. X indicates the average value. *$P < 0.01$; **$P < 0.001$. HTGL, hepatic triglyceride lipase.

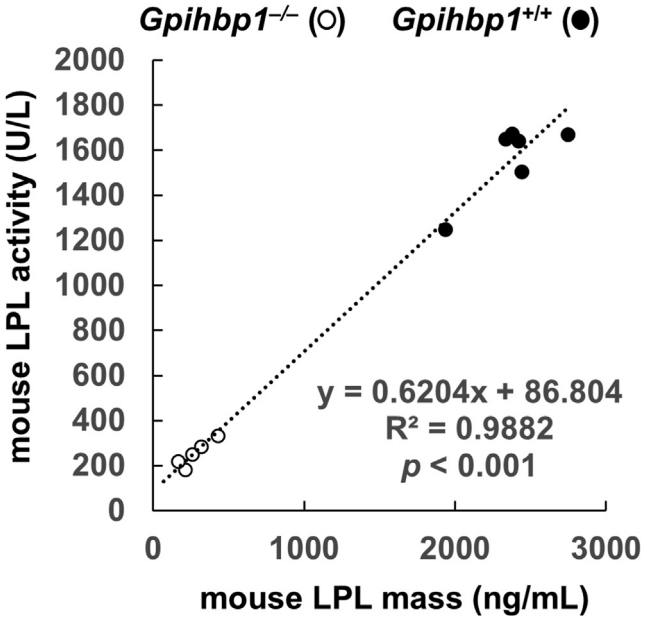

Fig. 5. Correlation between LPL mass and activity in post-heparin plasma samples from *Gpihbp1*$^{+/+}$ and *Gpihbp1*$^{-/-}$ mice. LPL mass and activity measurements were positively correlated both in *Gpihbp1*$^{+/+}$ and *Gpihbp1*$^{-/-}$ mice.

Post-heparin plasma levels of HTGL activity increased in both *Gpihbp1*$^{+/+}$ and *Gpihbp1*$^{-/-}$ mice (Fig. 4D). Before heparin, HTGL activity levels in *Gpihbp1*$^{+/+}$ mice (272.3 ± 27.0 U/L) were lower than in *Gpihbp1*$^{-/-}$ mice (446.3 ± 43.1 U/L) (Fig. 4D). After heparin, no significant differences in HTGL activity levels were observed in *Gpihbp1*$^{+/+}$ mice (939.2 ± 48.1 U/L) and *Gpihbp1*$^{-/-}$ mice (796.0 ± 82.4 U/L) (Fig. 4D).

DISCUSSION

In the current study, we developed a sandwich ELISA to measure mouse LPL. To the best of our knowledge, our mAb-based ELISA for mouse LPL is the first to be described. The ELISA accurately quantifies levels of LPL in mouse plasma samples. In our hands, the levels of LPL mass in pre-heparin plasma of mice were comparable to those in humans (3). The ELISA is sensitive and therefore can quantify LPL levels in the pre-heparin plasma—even in *Gpihbp1*$^{-/-}$ mice, where the pre-heparin plasma LPL levels are particularly low (20). We did not observe significant differences in the LPL activity levels in the pre-heparin plasma samples from *Gpihbp1*$^{+/+}$ and *Gpihbp1*$^{-/-}$ mice—even though LPL mass levels were significantly higher in *Gpihbp1*$^{+/+}$ mice than in *Gpihbp1*$^{-/-}$ mice. This observation is aligned with earlier studies showing that the LPL in pre-heparin plasma is predominantly in a catalytically inactive state (21).

Our LPL immunoassay revealed that the magnitude of the increase in plasma LPL levels after an infusion of heparin were greater in *Gpihbp1*$^{+/+}$ mice than in *Gpihbp1*$^{-/-}$ mice, as noted previously (20). In both lines of mice, we observed a correlation between LPL mass and activity levels in the post-heparin plasma, as is the case in humans (22).

Heparin treatment increased HTGL activity levels in both *Gpihbp1*$^{+/+}$ and *Gpihbp1*$^{-/-}$ mice. In the absence of heparin treatment, plasma HTGL activity levels were higher in *Gpihbp1*$^{-/-}$ mice than in *Gpihbp1*$^{+/+}$ mice. The mechanisms for the higher HTGL activity levels in *Gpihbp1*$^{-/-}$ mice are unclear but could conceivably reflect compensation for reduced intravascular LPL levels in *Gpihbp1*$^{-/-}$ mice.

In conclusion, we developed a specific and sensitive sandwich ELISA for measuring mouse LPL levels. This ELISA will prove useful for in vivo and in vitro research studies on intravascular lipolysis in mouse models.

Data availability

All data are contained within the manuscript.

Supplemental data

This article contains supplemental data.

Acknowledgments

The authors thank Mayumi Nishiyama for technical assistance.

Author contributions

M. P., S. G. Y., A. P. B., K. N., and M. M. conceptualization; T. K., K. M., I. F., K. F., K. O., E. Y., M. P., Y. Y., W. S., and A. P. B. data curation; K. M., I. F., M. P., Y. Y., W. S., and A. P. B. validation; K. M., I. F., M. P., Y. Y., W. S., and A. P. B. methodology; T. K., K. T., and T. N. writing–original draft; M. P., S. G. Y., A. P. B., K. N., and M. M. project administration; M. P., S. G. Y., A. P. B., K. N., and M. M. writing–review and editing; M. P., S. G. Y., A. P. B., K. N., and M. M. resources; M. P., S. G. Y., A. P. B., K. N., and M. M. supervision.

Author ORCIDs

Takao Kimura https://orcid.org/0000-0002-0941-2525
Kazuya Miyashita https://orcid.org/0000-0002-3783-1452
Michael Ploug https://orcid.org/0000-0003-2215-4265
Ye Yang https://orcid.org/0000-0003-4260-7700
Anne P. Beigneux https://orcid.org/0000-0002-7892-150X
Masami Murakami https://orcid.org/0000-0001-8795-5712

Funding and additional information

This work was supported by grants from the NHLBI [HL087228, HL146358, HL139725]; an American Heart Association Grant Postdoctoral Fellowship [834131]; a Leducq Foundation Network Grants [19CVD04, 23CVD02]; and a NOVO Nordisk Foundation Grant [NNF20OC0063444]. This work was also supported, by Grants-in-Aid scientific research from the Ministry of Education, Culture, Sports, Science and Technology of Japan [20KK0190, 22H02965 to M. M., 20K07841, 23K08003 to T. K.].

Conflict of interest

The authors declare that they have no conflicts of interest with the contents of this article.

Abbreviations

BSA, bovine serum albumin; GPIHBP1, glycosylphosphatidylinositol-anchored high-density lipoprotein binding protein 1; HTGL, hepatic triglyceride lipase; LPL, lipoprotein lipase; mAb, monoclonal antibody; mLPL, mouse LPL; QC, quality control.

Manuscript received May 9, 2023, and in revised form March 3, 2024. Published, JLR Papers in Press, , https://doi.org/10.1016/j.jlr.2024.100532

REFERENCES

1. Havel, R. J. (2010) Triglyceride-rich lipoproteins and plasma lipid transport. *Arterioscler. Thromb. Vasc. Biol.* **30**, 9–19
2. Young, S. G., Fong, L. G., Beigneux, A. P., Allan, C. M., He, C., Jiang, H., *et al.* (2019) GPIHBP1 and lipoprotein lipase, partners in plasma triglyceride metabolism. *Cell Metab.* **30**, 51–65
3. Shirakawa, T., Nakajima, K., Yatsuzuka, S., Shimomura, Y., Kobayashi, J., Machida, T., *et al.* (2015) The role of plasma lipoprotein lipase and adiponectin on the particle size of remnant lipoproteins in patients with diabetes mellitus and metabolic syndrome. *Clin. Chim. Acta.* **440**, 123–132
4. Machida, T., Miyashita, K., Sone, T., Tanaka, S., Nakajima, K., Saito, M., *et al.* (2015) Determination of serum lipoprotein lipase using a latex particle-enhanced turbidimetric immunoassay with an automated analyzer. *Clin. Chim. Acta.* **442**, 130–135
5. Miyashita, K., Fukamachi, I., Nagao, M., Ishida, T., Kobayashi, J., Machida, T., *et al.* (2018) An enzyme-linked immunosorbent assay for measuring GPIHBP1 levels in human plasma or serum. *J. Clin. Lipidol.* **12**, 203–210
6. Weinstein, M. M., Yin, L., Beigneux, A. P., Davies, B. S. J., Gin, P., Estrada, K., *et al.* (2008) Abnormal patterns of lipoprotein lipase release into the plasma in GPIHBP1-deficient mice. *J. Biol. Chem.* **283**, 34511–34518
7. Gårdsvoll, H., Hansen, L. V., Jørgensen, T. J., and Ploug, M. (2007) A new tagging system for production of recombinant proteins in Drosophila S2 cells using the third domain of the urokinase receptor. *Protein Expr. Purif.* **52**, 384–394
8. Winther, A. M. L., Kristensen, K. K., Kumari, A., and Ploug, M. (2021) Expression and one-step purification of active LPL contemplated by biophysical considerations. *J. Lipid Res.* **62**, 100149
9. Leth-Espensen, K. Z., Kristensen, K. K., Kumari, A., Winther, A. L., Young, S. G., Jørgensen, T. J. D., *et al.* (2021) The intrinsic instability of the hydrolase domain of lipoprotein lipase facilitates its inactivation by ANGPTL4-catalyzed unfolding. *Proc. Natl. Acad. Sci. U. S. A.* **118**, e2026650118
10. Mysling, S., Kristensen, K. K., Larsson, M., Beigneux, A. P., Gårdsvoll, H., Fong, L. G., *et al.* (2016) The acidic domain of the endothelial membrane protein GPIHBP1 stabilizes lipoprotein lipase activity by preventing unfolding of its catalytic domain. *Elife.* **5**, e12095
11. Allan, C. M., Larsson, M., Hu, X., He, C., Jung, R. S., Mapar, A., *et al.* (2016) An LPL-specific monoclonal antibody, 88B8, that abolishes the binding of LPL to GPIHBP1. *J. Lipid Res.* **57**, 1889–1898
12. Kristensen, K. K., Leth-Espensen, K. Z., Mertens, H. D. T., Birrane, G., Meiyappan, M., Olivecrona, G., *et al.* (2020) Unfolding of monomeric lipoprotein lipase by ANGPTL4: Insight into the regulation of plasma triglyceride metabolism. *Proc. Natl. Acad. Sci. U. S. A.* **117**, 4337–4346
13. Kristensen, K. K., Midtgaard, S. R., Mysling, S., Kovrov, O., Hansen, L. B., Skar-Gislinge, N., *et al.* (2018) A disordered acidic domain in GPIHBP1 harboring a sulfated tyrosine regulates lipoprotein lipase. *Proc. Natl. Acad. Sci. U. S. A.* **115**, E6020–E6029
14. Imamura, S., Kobayashi, J., Nakajima, K., Sakasegawa, S., Nohara, A., Noguchi, T., *et al.* (2008) A novel method for measuring human lipoprotein lipase and hepatic lipase activities in post-heparin plasma. *J. Lipid Res.* **49**, 1431–1437
15. Nakajima, K., Machida, T., Imamura, S., Kawase, D., Miyashita, K., Fukamachi, I., *et al.* (2018) An automated method for measuring lipoprotein lipase and hepatic triglyceride lipase activities in post-heparin plasma. *Clin. Chim. Acta.* **487**, 54–59
16. Kimura, N., Kikumori, A., Kawase, D., Okano, M., Fukamachi, K., Ishida, T., *et al.* (2019) Species differences in lipoprotein lipase and hepatic lipase activities: a comparative studies of animal models of lifestyle-related diseases. *Exp. Anim.* **68**, 267–275
17. Birrane, G., Beigneux, A. P., Dwyer, B., Strack-Logue, B., Kristensen, K. K., Francone, O. L., *et al.* (2019) Structure of the lipoprotein-GPIHBP1 complex that mediates plasma triglyceride hydrolysis. *Proc. Natl. Acad. Sci. U. S. A.* **116**, 1723–1732
18. Wayne, P. A. (2004) CLSI EP5-A2 Protocol. Evaluation of Precision Performance of Quantitative Measurement Methods. Approved Guidelines 2nd ed,. **24**. Clinical and Laboratory Standards Institute (CLSI), Berwyn, PA
19. Wayne, P. A. (2004) CLSI EP17-A protocol. Protocols For Determination of Limits of Detection and Limits of Quantitation. Approved Guidelines 2nd ed,. **24**. Clinical and Laboratory Standards Institute (CLSI), Berwyn, PA
20. Beigneux, A. P., Davies, B. S., Gin, P., Weinstein, M. M., Farber, E., Qiao, X., *et al.* (2007) Glycosylphosphatidylinositol-anchored high-density lipoprotein binding protein 1 plays a critical role in the lipolytic processing of chylomicrons. *Cell Metab.* **5**, 279–291
21. Dallinga-Thie, G. M., Zonneveld-de Boer, A. J., van Vark-van der Zee, L. C., van Haperen, R., van Gent, T., Jansen, H., *et al.* (2007) Appraisal of hepatic lipase and lipoprotein lipase activities in mice. *J. Lipid Res.* **48**, 2788–2791
22. Sato, K., Okajima, F., Miyashita, K., Imamura, S., Kobayashi, J., Stanhope, K., *et al.* (2016) Most lipoorotein lipase is bound to remnant lipoproteins in plasma: a new definition for remnant lipoproteins. *Clin. Chim. Acta.* **461**, 114–125